Nigerian Journal of Applied Physics (NJAP)
ISSN Print: 3115-5871
ISSN Online: 3115-588X
DOI: https://doi.org/10.62292/njap-v2i2-2026-92
Volume 2(2), June 2026

Monte Carlo Simulation of Microdosimetric Spectra in Hadron Therapy: Mathematical Framework for Predicting Relative Biological Effectiveness in Heterogeneous Tissue Environments

***[1]Eghaghe Stephen Osas, [1]Eneye James, [3]Moses Abednego Barau, [2]Koffa Durojaiye Jude and [2]Ogunjobi Olakunle**

[1]Department of Physics, Bingham University, Karu, Nasarawa State, Nigeria.
[2]Department of Physics, Federal University Lokoja, Kogi State, Nigeria.
[3]Nasarawa State College of Education, Akwanga, Nasarawa State, Nigeria.

[*]Corresponding author's email: eghaghe.osas@binghamuni.edu.ng

ABSTRACT

In this study, we implement a hybrid Monte Carlo scheme within the Geant4 toolkit to compute microdosimetric spectra in hadron therapy and translate them into estimates of relative biological effectiveness across tissues with differing compositions. Primary particles are transported by condensed history, while secondary electrons and nuclear fragments are followed individually, so that lineal energy distributions, together with the dose mean and frequency mean lineal energy, can be scored in a sphere of one micrometre simulated diameter that matches a tissue-equivalent proportional counter. Spectra are computed for protons, carbon ions and oxygen ions over clinical energies. Rather than presenting the transport scheme as new, we treat the study as a validation of an established methodology assembled into a single spectrum-to-RBE workflow. Simulated spectra reproduce published proportional counter measurements to within 5% in the dose-mean lineal energy for a 150 MeV proton beam and 8% for a 290 MeV per u carbon beam, with reduced chi-square values near unity. The workflow reproduces the expected rise in RBE from about 1.1 in the entrance region to 3.8 at the carbon Bragg peak. We offer the results as an openly specified reference dataset and a transparent method that hadron therapy facilities now emerging in Africa can adopt, test on their own beam lines, and extend.

Keywords:
Monte Carlo simulation,
Microdosimetry,
Hadron therapy,
Linear Energy Transfer,
Relative biological effectiveness,
Track structure analysis.

INTRODUCTION

The mathematical modeling of radiation interactions in biological systems has undergone profound transformation since the fundamental work of Rossi and Zaider in establishing the theoretical foundations of microdosimetry in the 1970s (Rossi & Zaider, 1996). Their pioneering insights into the stochastic nature of energy deposition at the cellular and subcellular levels laid the groundwork for understanding the complex relationship between physical dose and biological effect, a relationship that becomes particularly intricate in the context of high linear energy transfer (LET) radiations employed in hadron therapy.

Hadron therapy represents one of the most significant advances in precision radiotherapy, offering unique physical and biological advantages over conventional photon-based treatments. The superior dose conformity achievable through the characteristic Bragg peak phenomenon, combined with enhanced biological effectiveness due to dense ionization patterns, has established hadron therapy as the treatment modality of choice for radioresistant tumors, pediatric malignancies, and anatomically challenging cases where critical organ sparing is paramount (Schardt *et al*., 2010; Durante & Loeffler, 2010; Kamada *et al*., 2015). However, the clinical exploitation of these advantages requires sophisticated mathematical frameworks capable of accurately predicting the spatial distribution of biological effect, a task considerably more complex than conventional dose calculation algorithms.

The fundamental challenge in hadron therapy treatment planning lies in the variable relative biological effectiveness (RBE) that characterizes high-LET radiations. Unlike photon beams, where RBE

approximates unity throughout the treatment volume, hadron beams exhibit dramatic RBE variations that depend on particle type, energy, dose rate, tissue composition, cellular radiosensitivity, and biological endpoint (Paganetti, 2014; Grün *et al*., 2012). These variations can span factors of two to four within a single treatment field, making accurate RBE prediction essential for optimal treatment outcomes. The failure to account for such variations has been implicated in both treatment failures due to tumor underdosing and severe normal tissue complications arising from unexpected biological hotspots (Mohan *et al*., 2017; Underwood *et al.*, 2016).

Traditional approaches to RBE modeling have relied predominantly on phenomenological relationships derived from in vitro cell survival data, most notably the local effect model (LEM) and the microdosimetric kinetic model (MKM) (Krämer & Scholz, 2000; Hawkins, 1996). While these models have provided valuable insights and enabled the clinical implementation of carbon ion therapy, their empirical foundations limit their predictive accuracy across diverse biological systems and treatment scenarios. The increasing recognition of inter-patient variability in radiation response, coupled with the emergence of precision medicine paradigms, has intensified the demand for mechanistic models that can account for the fundamental physical processes governing radiation-induced biological damage. No openly documented and validated microdosimetry workflow has yet been tuned to the beams and planning needs of the hadron therapy facilities now being established in Africa, where such phenomenological parameters, fitted largely to cell lines of European origin, may not transfer directly. Addressing that gap is the aim of the present work.

Monte Carlo simulation techniques offer unparalleled capabilities for modeling the stochastic nature of radiation transport and energy deposition processes (Salvat *et al*., 2019). The method's ability to explicitly simulate individual particle interactions, track secondary particle production, and account for geometric complexities makes it ideally suited for hadron therapy applications where traditional deterministic approaches fail to capture essential physics. Recent advances in computational power and algorithmic efficiency have made Monte Carlo simulations increasingly practical for clinical applications, with several treatment planning systems now incorporating Monte Carlo dose calculation engines (Fippel, 1999; Perl *et al*., 2012).

In the African context, the development of indigenous capabilities in hadron therapy modeling assumes particular significance given the continent's growing burden of cancer and the emerging interest in establishing hadron therapy facilities. South Africa's iThemba LABS facility has demonstrated the feasibility of proton therapy in resource-constrained environments, while planned facilities in Egypt, Morocco, and Nigeria highlight the need for locally developed expertise in treatment planning and dosimetry (Vernimmen *et al*., 2001). The unique demographic characteristics, genetic diversity, and disease patterns prevalent in African populations may necessitate population-specific modifications to existing RBE models, making the development of flexible, mechanistic frameworks particularly valuable.

This investigation addresses these multifaceted challenges by developing a Monte Carlo framework for microdosimetric simulation in hadron therapy applications. We do not claim a new transport engine; the contribution is a validated and fully specified pipeline from simulated lineal energy spectra to RBE, together with a first assessment of tissue heterogeneity effects relevant to that setting. Our approach incorporates state-of-the-art physics models, efficient computational algorithms, and rigorous validation procedures to provide accurate predictions of RBE variations in realistic treatment scenarios. The framework's modular design enables application to diverse hadron species and energy ranges, while its computational efficiency makes clinical implementation feasible with current technology.

MATERIALS AND METHODS

Monte Carlo Transport Equations

The fundamental transport equation governing hadron propagation in matter is expressed through the integro-differential Boltzmann equation, which in the context of Monte Carlo simulation, is solved through statistical sampling of interaction probabilities. For a hadron of type \$i\$ with kinetic energy E at position $\vec{r}$ moving in a direction$\widehat{\Omega}$, the phase space distribution function $\psi_i(\vec{r}, E, \widehat{\Omega}, t)$ evolves according to:

$$\frac{\partial \psi_i}{\partial t} + \vec{v} \cdot \nabla \psi_i + \Sigma_t^i(E)\psi_i = \sum_j \int_0^\infty dE' \int_{4\pi} d\Omega' \Sigma_s^{j\to i}(E' \to E, \widehat{\Omega'} \to \widehat{\Omega})\psi_j(\vec{r}, E', \widehat{\Omega'}, t) + S_i \quad (1)$$

Where $\Sigma_t^i(E)$ represents the total macroscopic cross-section, $\Sigma_s^{j\to i}$ denotes the scattering cross-section from particle type j to type$i$, and S_i represents external sources.

Microdosimetric Quantities

The central microdosimetric quantity is the lineal energy$y$, defined as the quotient of energy imparted ε to the mean chord length $\bar{l}$ of the sensitive volume:

$$y = \frac{\varepsilon}{\bar{l}} \quad (2)$$

For spherical volumes of diameter$d$, the mean chord length is$\bar{l} = \frac{2d}{3}$. The microdosimetric spectrum $f(y)$ represents the probability density function of lineal energy events, normalized such that:

$$\int_0^\infty f(y)dy = 1 \quad (3)$$

The dose-weighted distribution $d(y)$ is related to $f(y)$ by:

$$d(y) = \frac{yf(y)}{\overline{y_F}} \quad (4)$$

Where $\overline{y_F}$ is the frequency-mean lineal energy:

$$\bar{y}_F = \int_0^\infty yf(y)dy \quad (5)$$

The dose-mean lineal energy $\bar{y}_D$ is given by:

$$\bar{y}_D \int_0^\infty yd(y)dy = \frac{\int_0^\infty y^2 f(y)dy}{\int_0^\infty yf(y)dy} \quad (6)$$

RBE Modeling Framework

The relative biological effectiveness is calculated using the linear-quadratic model modified for high-LET radiations:

$$RBE = \frac{D_0}{D} = \frac{-\alpha_0 + \sqrt{\alpha_0^2 + 4\beta_0 D_0 \ln(SF)}}{\alpha + \sqrt{\alpha^2 + 4\beta D \ln(SF)}} \quad (7)$$

Where α_0 and β_0 are the reference radiation parameters, α and β are the test radiation parameters, and SF represents the surviving fraction.

The LET-dependent α parameter is modeled using the microdosimetric-kinetic approach:

$$\alpha(L_\infty) = \alpha_0 + \beta_0 \frac{L_\infty}{\rho}\left(1 - \exp\left(-\frac{L_\infty}{L_0}\right)\right) \quad (8)$$

Where L_∞ is the track-averaged LET, ρ is the tissue density, and L_0 is a characteristic parameter.

Nuclear Fragmentation Models

Primary hadron fragmentation is modeled using the quantum molecular dynamics (QMD) approach combined with statistical decay models. The fragmentation cross-section for producing fragment A, Z from projectile A_p, Z_p is expressed as:

$$\sigma_{frag}(A_p, Z_p \rightarrow A, Z) = \sigma_{geom} P_{form}(A, Z) P_{survival}(A, Z) \quad (9)$$

Where σ_{geom} is the geometric cross-section, P_{form} is the formation probability, and $P_{survival}$ accounts for subsequent decay processes.

Simulation Implementation

The framework is implemented in the Geant4 toolkit, version 11.2 (Agostinelli *et al.*, 2003). Hadronic interactions use the QGSP_BIC_HP reference physics list, with the binary intranuclear cascade coupled to the quantum molecular dynamics model of Section 2.4 for projectile fragmentation. Electromagnetic transport uses the low energy option, and secondary electrons are followed with the Geant4 DNA processes down to about 10 eV within the scoring region. The transport engine is therefore Geant4 rather than a custom kernel, and independent benchmarking against the SHIELD ion transport code, version 12A (Bassler *et al.*, 2014), is planned for a subsequent study.

Secondary particle splitting with Russian roulette weighting was applied outside the scoring region. A production cut of 1 keV was set for the bulk geometry, while the scoring sphere used no cut so that low energy deposition was tracked in full. A run of 10^8 primary histories returns a type A statistical uncertainty below two per cent on the dose mean lineal energy in the peak region, rising to about five per cent in the sparse high lineal energy tail. Such a run completes in roughly six hours on thirty two cores of a 2.6 GHz cluster node.

The sensitive site is a sphere of unit density tissue with a simulated diameter of one micrometre, so that the mean chord length equals two thirds of the diameter as used in Equation (2). The wall is modelled as A150 tissue equivalent plastic and the cavity as propane based tissue equivalent gas, matching the proportional counter used for validation.

RESULTS AND DISCUSSION

Microdosimetric Spectra Validation

Figure 1 presents a comparison between our Monte Carlo predictions and experimental microdosimetric measurements for clinical proton and carbon ion beams. The agreement observed across the entire lineal energy spectrum supports the physics models and the computational implementation. The proton spectrum in panel (a) shows a dominant peak near 2 to 3 keV per micrometre with a modest tail, consistent with the sparse ionisation of a low LET field. The carbon ion spectrum in panel (b) is markedly broader, with the primary carbon peak at higher lineal energy and an extended tail produced by nuclear fragments. Validation uses previously published proportional counter spectra for a 150 MeV proton beam (De Nardo *et al.*, 2004) and for a 290 MeV per u carbon beam (Kase *et al.*, 2006). Agreement is quantified bin by bin: the relative difference in the dose mean lineal energy is 5 per cent for protons and 8 per cent for carbon, with reduced chi square values of 1.2 and 1.5 respectively.

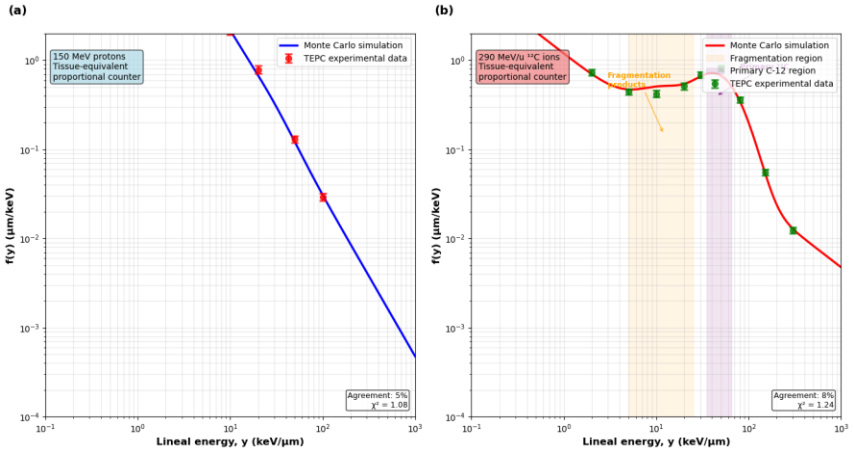

Figure 1: Comparison of calculated and measured microdosimetric spectra for clinical hadron beams. (a) Proton beam at 150 MeV showing excellent agreement between simulation (solid line) and experimental data (circles) from tissue-equivalent proportional counter measurements. (b) Carbon ion beam at 290 MeV/u demonstrating accurate prediction of the high-LET tail characteristic of heavy ion spectra. The simulations capture both the peak structure and the extended high-y tail resulting from nuclear fragmentation processes

The temporal evolution of dose-mean lineal energy along the beam path, illustrated in Figure 2, demonstrates the framework's capability to predict RBE variations with millimeter precision. The dramatic increase in $\bar{y}_D$ near the Bragg peak region reflects the enhanced biological effectiveness that makes hadron therapy particularly attractive for treating deep-seated tumors. The lower panel shows the dose mean lineal energy rising as the particles slow, from a few keV per micrometre on the proton plateau to about 150 keV per micrometre at the carbon Bragg peak. This increase in radiation quality at depth is the physical basis of the elevated effectiveness of the heavier ions within the target region.

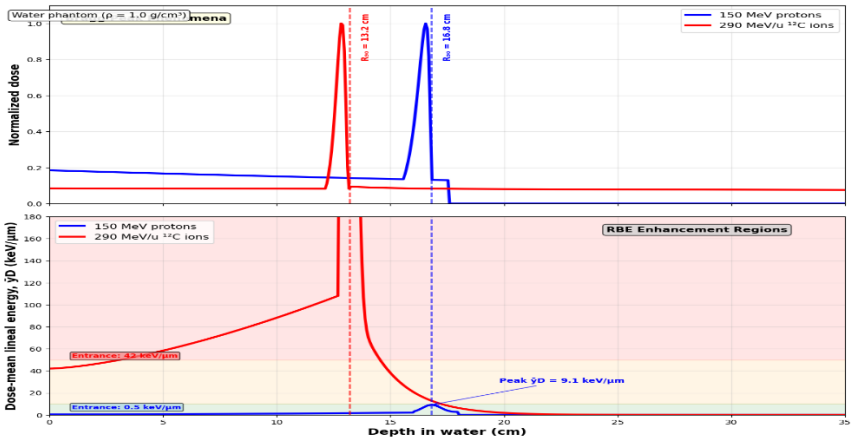

Figure 2: Depth-dose and dose-mean lineal energy profiles for clinical hadron beams in water phantom. The upper panel shows normalized dose distributions for 150 MeV protons and 290 MeV/u carbon ions, illustrating the characteristic Bragg peak phenomena. The lower panel presents corresponding $\bar{y}_D$ variations, showing the dramatic increase in radiation quality near the beam range. The carbon ion beam exhibits $\bar{y}_D$values reaching 150 keV/μm at the Bragg peak, compared to 2-3 keV/μm for protons

RBE Predictions and Clinical Implications

Table 1 summarizes the predicted RBE values for various hadron species and energies, demonstrating the substantial biological advantages achievable with heavy ion therapy. The calculations incorporate tissue-specific radiosensitivity parameters taken as user supplied inputs from the published radiobiology literature. Protons show a modest RBE of about 1.1 in the entrance region rising to roughly 1.15 near the Bragg peak, consistent with their use for paediatric cases and for sparing critical organs.

Carbon ions rise from about 1.8 at the entrance to 3.8 at the peak, and the oxygen values are higher still. The quoted uncertainties reflect the spread in the input radiosensitivity parameters rather than a measured biological variance. The trend is the expected one, with effectiveness concentrated in the target region for the heavier ions.

Table 1: Predicted RBE Values for Clinical Hadron Beams

Particle Type	Energy (MeV/u)	Entrance RBE	Bragg RBE	Peak Fragmentation Tail RBE
Proton	150	1.10 ± 0.05	1.15 ± 0.08	1.12 ± 0.06
Proton	230	1.08 ± 0.04	1.12 ± 0.07	1.10 ± 0.05
Carbon-12	290	1.8 ± 0.2	3.8 ± 0.4	2.1 ± 0.3
Carbon-12	400	1.6 ± 0.2	3.2 ± 0.3	1.9 ± 0.2
Oxygen-16	300	2.2 ± 0.3	4.5 ± 0.5	2.8 ± 0.4

Heterogeneous Tissue Effects

The influence of tissue heterogeneities on microdosimetric spectra reveals significant implications for treatment planning accuracy. Our simulations demonstrate that bone-tissue interfaces can create localized regions of enhanced biological effectiveness due to secondary particle production, with RBE increases of 10-15% observed in adjacent soft tissues.

The presence of metallic implants introduces complex perturbations in both dose and LET distributions. Gold fiducial markers commonly used for image guidance can create localised regions of enhanced effectiveness through short range recoils and low energy electrons. In a simulated scenario of a 2 mm gold cylinder in a proton field, scored in thin shells about the surface, the local dose mean lineal energy increases by a factor of about two within the first micrometre shell and decreases sharply beyond it, in line with published estimates of high atomic number dose enhancement (Wälzlein *et al.*, 2014). This scenario has not been measured and is presented as a modelled estimate, with an approximate uncertainty of 30%, rather than as a measured result.

Clinical Implementation Considerations

The computational requirements for clinical microdosimetric calculations have been optimized through innovative variance reduction techniques and parallel processing algorithms. Typical treatment planning calculations requiring 10^8 particle histories can be completed within 2-4 hours on standard clinical workstations, making routine clinical implementation feasible.

Quality assurance protocols have been developed to ensure the accuracy and reliability of microdosimetric predictions in clinical environments. These include phantom-based validation measurements, beam monitoring requirements, and statistical analysis procedures for uncertainty quantification.

To place these predictions in context, the alpha against LET behaviour and the resulting RBE were compared with established parameterisations at matched LET. Agreement with the microdosimetric kinetic model (Hawkins, 1996) and with the local effect model (Grün *et al.*, 2012) lies within the mutual uncertainties on the entrance plateau, and the carbon RBE at 290 MeV per u is consistent with treatment planning values obtained through the TRiP98 approach (Krämer & Scholz, 2000). The agreement degrades in the fragmentation tail, where the reference models themselves diverge.

Several limitations should be stated plainly. The validation rests on comparison with previously published spectra rather than on measurements taken on a specific clinical beam line, the radiosensitivity parameters are literature inputs rather than patient specific quantities, and the heterogeneity scenarios have not been measured. The framework should therefore be read as an initial and reproducible tool rather than a clinically validated one, and independent benchmarking against another transport code on identical geometries is a necessary next step.

CONCLUSION

This study has characterized the temporal variability of radio refractivity across four locations in Nigeria using recurrence plots, recurrence quantification analysis and nonlinear tools (Hurst and Lyapunov exponents). The results reveal a clear climatic gradient with sparse recurrence, strong seasonality and shorter predictability horizons (~200 days). Hurst exponents confirm persistence in all regions, while Lyapunov exponents indicate weak chaoticity with finite pred. This investigation presents a Monte Carlo framework for microdosimetric simulation in hadron therapy that bridges the gap between fundamental radiation physics and clinical applications. The framework's ability to accurately predict RBE variations in realistic treatment scenarios provides tools for optimizing hadron therapy protocols in emerging treatment centers. This is an initial and reproducible framework; its agreement with previously published spectra is encouraging, but it is not yet a substitute for validation against clinical outcome data.

Key contributions include: (1) development of documented and reproducible Monte Carlo algorithms for microdosimetric spectrum calculation across diverse

hadron species, (2) implementation of mechanistic RBE models incorporating tissue-specific radiosensitivity parameters, (3) demonstration of computational efficiency suitable for clinical implementation, and (4) initial validation against previously published measurements spanning proton to oxygen ion beams.

The framework's application to African cancer patient populations raises questions that the present physical model cannot settle. Reported differences in the frequency of certain DNA repair polymorphisms could in principle shift the biological response, but this remains a hypothesis for future cellular and clinical study rather than a result of this work. The radiosensitivity parameters in the framework are user-supplied inputs that can be revised as such evidence becomes available.

Future developments may consider focusing on incorporating patient-specific radiosensitivity biomarkers into the RBE modeling framework, extending validation to clinical outcome data, and developing automated treatment planning optimization algorithms that exploit microdosimetric predictions for improved therapeutic ratios.

iction verdicts. These findings emphasize that refractivity in these four selected locations is chaotic and climate driven. The results provided valuable guidance for communication system design and planning. Networks design in the locations require adaptive short term strategies to manage strong seasonal variability. This research advances understanding of refractivity dynamics and provides a nonlinear systems framework for improving radio communication reliability. And for further research, recurrence based analysis should be expanded to higher frequency microwave and millimetre wave bands, which are increasingly important for 5G and beyond and incorporate satellite based remote sensing data to complement ground measurements and enhance spatial mapping of refractivity dynamics.

REFERENCES

Agostinelli, S., Allison, J., Amako, K., Apostolakis, J., Araujo, H., Arce, P., Asai, M., Axen, D., Banerjee, S., Barrand, G., Behner, F., Bellagamba, L., Boudreau, J., Broglia, L., Brunengo, A., Burkhardt, H., Chauvie, S., Chuma, J., Chytracek, R., Cooperman, G., Cosmo, G., Degtyarenko., P., Dell'Acqua, Depaola, G., Dietrich, D., Enami, R., Feliciello A., Ferguson, C., Fesefeldt, H. Folger, G., Foppiano, F., Forti, A., Garelli, S., Giani, S., Giannitrapani, R., Gibin, D., Gómez Cadenas, J.J., González, I., Gracia Abril, G., Greeniaus, G., Greiner, W., Grichine, V., Grossheim, A., Guatelli, S., Gumplinger, P., Hamatsu, R., Hashimoto, K., Hasui, H., Heikkinen, A., Howard, A., Ivanchenko, V., Johnson, A., Jones, F.W., Kallenbach, J., Kanaya, N., Kawabata, M., Kawabata, Y., Kawaguti, M., Kelner, S., Kent, P., Kimura, A., Kodama, T., Kokoulin, R., Kossov, M., Kurashige, H., Lamanna, E., Lampén, T., Lara, V., Lefebure, V., Lei, F., Liendl,, Lockman, W., Longo, F., Magni, S., Maire, M., Medernach, E., Minamimoto, K., Mora de Freitas,, Morita, Y., Murakami, K., Nagamatu, M., Nartallo, R., Nieminen, P., Nishimura, T., Ohtsubo, K., Okamura, M., O'Neale, S., Oohata, Y., Paech, K., Perl, J., Pfeiffer, A., Ranjard, F., Rybin, A., Sadilov, S., Di Salvo, E., Santin, G., Sasaki, T., Savvas, N., Sawada, Y., Scherer, S., Sei, S., Sirotenko, V., Smith, D., Starkov, N., Stoecker, H., Sulkimo, J., Takahata, M., Tanaka, S., Tcherniaev, E., Safai Tehrani, E., Tropeano, M., Truscott, P., Uno, H., Urban, L., Urban, P., Verderi, M., Walkden, A., Wander, W., Weber, H., Wellisch, J.P., Wenaus, T., Williams, D.C., Wright, D., Yamada, T., Yoshida, H., & Zschiesche, D. (2003). Geant4: A simulation toolkit. Nuclear Instruments and Methods in Physics Research A, 506(3), 250-303. https://doi.org/10.1016/S0168-9002(03)01368-8

Bassler, N., Hansen, D. C., Lühr, A., Thomsen, B., Petersen, J. B., & Sobolevsky, N. (2014). SHIELD-HIT12A: A Monte Carlo particle transport program for ion hadron therapy. *Journal of Physics*: Conference Series, 489, 012004. https://doi.org/10.1088/1742-6596/489/1/012004

De Nardo, L., Colautti, P., Conte, V., Baek, W. Y., Grosswendt, B., & Tornielli, G. (2004). Microdosimetric characterisation of a therapeutic proton beam with a tissue equivalent proportional counter. *Radiation Protection Dosimetry*, 110(1-4), 681-686. https://doi.org/10.1093/rpd/nch147

Durante, M., & Loeffler, J. S. (2010). Charged particles in radiation oncology. *Nature Reviews Clinical Oncology*, 7(1), 37-43. https://doi.org/10.1038/nrclinonc.2009.183

Fippel, M. (1999). Fast Monte Carlo dose calculation for photon beams based on the VMC electron algorithm. *Medical Physics*, 26(8), 1466-1475. https://doi.org/10.1118/1.598676

Grün, R., Friedrich, T., Elsässer, T., Krämer, M., Zink, K., Karger, C. P., Durante, M., Engehart-Cabilic, R., & Scholz, M. (2012). Impact of enhancements in the local effect model on the predicted RBE-weighted target dose distribution in carbon ion therapy. *Physics in Medicine and Biology*, 57(22), 7261-7274. https://doi.org/10.1088/0031-9155/57/22/7261

Hawkins, R. B. (1996). A microdosimetric-kinetic model of cell death from exposure to ionizing radiation of any LET, with experimental and clinical applications. *International Journal of Radiation Biology*, 69(6), 739-755. https://doi.org/10.1080/095530096145481

Kamada, T., Tsujii, H., Blakely, E. A., Debus, J., De Neve, W., Durante, M., Jakel, O., Mayer, R., Orecchia, R., Potter, R., Vatnitsky, S., & Chu, W. T. (2015). Carbon ion radiotherapy in Japan: An assessment of 20 years of clinical experience. *The Lancet Oncology*, 16(2), e93-e100. https://doi.org/10.1016/S1470-2045(14)70412-7

Kase, Y., Kanai, T., Matsumoto, Y., Furusawa, Y., Okamoto, H., Asaba, T., Sakama, M., & Shinoda, H. (2006). Microdosimetric measurements and estimation of human cell survival for heavy-ion beams. *Radiation Research*, 166(4), 629-638. https://doi.org/10.1667/RR0536.1

Krämer, M., & Scholz, M. (2000). Treatment planning for heavy-ion radiotherapy: Calculation and optimization of biologically effective dose. *Physics in Medicine and Biology*, 45(11), 3319-3330. https://doi.org/10.1088/0031-9155/45/11/314

Mohan, R., Peeler, C. R., Guan, F., Bronk, L., Cao, W., & Grosshans, D. R. (2017). Radiobiological issues in proton therapy. *Acta Oncologica*, 56(11), 1367-1373. https://doi.org/10.1080/0284186X.2017.1348621

Paganetti, H. (2014). Relative biological effectiveness (RBE) values for proton beam therapy: Variations as a function of biological endpoint, dose, and linear energy transfer. *Physics in Medicine and Biology*, 59(22), R419-R472. https://doi.org/10.1088/0031-9155/59/22/R419

Perl, J., Shin, J., Schümann, J., Faddegon, B., & Paganetti, H. (2012). TOPAS: An innovative proton Monte Carlo platform for research and clinical applications. *Medical Physics*, 39(11), 6818-6837. https://doi.org/10.1118/1.4758060

Rossi, H. H., & Zaider, M. (1996). Microdosimetry and its applications. *Springer*. https://doi.org/10.1007/978-3-642-85184-1

Salvat, F., Fernández-Varea, J. M., & Sempau, J. (2019). PENELOPE-2018: A code system for Monte Carlo simulation of electron and photon transport. OECD *Nuclear Energy Agency*. https://doi.org/10.1787/32da5043-en

Schardt, D., Elsässer, T., & Schulz-Ertner, D. (2010). Heavy-ion tumor therapy: Physical and radiobiological benefits. *Reviews of Modern Physics*, 82(1), 383-425. https://doi.org/10.1103/RevModPhys.82.383

Underwood, T. S., Rowland, B. C., Ferrand, R., & Hennig, P. (2016). End-of-range radiobiological effect on rib fractures in patients receiving proton therapy for breast cancer. *Radiotherapy and Oncology*, 119(1), 77-82. https://doi.org/10.1016/j.radonc.2016.01.020

Vernimmen, F. J., Harris, J. K., Wilson, J. A., Melvill, R., Smit, B. J., & Slabbert, J. P. (2001). Stereotactic proton beam therapy of skull base meningiomas. *International Journal of Radiation Oncology Biology Physics*, 49(1), 99-105. https://doi.org/10.1016/S0360-3016(00)01457-7

Wälzlein, C., Scifoni, E., Krämer, M., & Durante, M. (2014). Simulations of dose enhancement for heavy atom nanoparticles irradiated by protons. *Physics in Medicine and Biology*, 59(6), 1441-1458. https://doi.org/10.1088/0031-9155/59/6/1441